D. Erkakan et al. / Hacettepe J. Biol. & Chem., 2022, 50 (4), 397-414

Research Article

Hacettepe Journal of Biology and Chemistry

journal homepage: www.hjbc.hacettepe.edu.tr

Green Synthesis of Silver Nanoparticles Using *Salvia Fruticosa* Mill. Extract and the Effect of Synthesis Parameters on Their Formation, Antioxidant, and Electro-Catalytic Activity

Gümüş Nanopartiküllerin *Salvia Fruticosa* Mill. Ekstresi Kullanılarak Yeşil Sentezi ve Sentez Parametrelerinin Oluşumları, Antioksidan ve Elektrokatalitik Aktiviteleri Üzerindeki Etkisi

Damla Erkakan[1], Neziha Yağmur Diker[2], Müşerref Önal[3] and İffet İrem Çankaya[2]

[1]Graduate School of Natural and Applied Sciences, Ankara University, Ankara, Turkey.

[2]Department of Pharmaceutical Botany, Faculty of Pharmacy, Hacettepe University, Ankara, Turkey.

[3]Department of Chemistry, Faculty of Science, Ankara University, Ankara, Turkey.

ABSTRACT

Among green synthesis methods, which are an eco-friendly, non-toxic, simple, and safe approach for the synthesis of silver nanoparticles (AgNPs), using plant extract is the most efficient method. *Salvia fruticosa* Mill. which was not used formerly was selected for this research. By changing the synthesis parameters (the amount of extract, extract concentration, and silver ion concentration in precursors), their effects on the formation and structure of nanoparticles were investigated by UV-visible spectroscopy, transmission electron microscopy and Fourier transform infrared spectroscopy techniques. The antioxidant activity of extracts and AgNPs was evaluated by performing DPPH (2,2 diphenyl-1-picrylhydrazyl) assay. It is observed that the phytosynthesized nanoparticles also possess antioxidant potentials. Finally, AgNPs were used as modifiers for carbon paste electrode (CPE) and their effect on charge transfer resistance and the ascorbic acid signal was investigated by using electrochemical impedance spectroscopy (EIS), cyclic voltammetry (CV), and square wave voltammetry (SWV). E1-1/CPE showed good electro-catalytic oxidation of ascorbic acid and can be utilized for the development of the new sensors. According to the results, in the process of green synthesis of AgNPs, synthesis parameters are vital as they change not only the size and size distribution of the AgNPs but also their antioxidant activity and electrochemical properties.

Key Words
Green chemistry, silver nanoparticles, *Salvia fruticosa* Mill., antioxidant activity.

ÖZ

Gümüş nanopartiküllerin (AgNP'ler) sentezi için çevre dostu, toksik olmayan, basit ve güvenli bir yaklaşım olan yeşil sentez yöntemleri arasında bitki ekstresi en etkili olanıdır. Bu araştırma için daha önce hiç kullanılmamış bir bitki olan *Salvia fruticosa* Mill. seçilmiştir. Sentez parametreleri (ekstre miktarı, ekstre konsantrasyonu ve öncüllerdeki gümüş iyon konsantrasyonu) değiştirilerek nanopartiküllerin oluşumu ve yapısı üzerindeki etkileri Ultraviyole ve görünür ışık spektroskopi, geçirimli elektron mikroskobu ve Fourier dönüşümlü kızılötesi spektroskopi teknikleri ile araştırılmıştır. Ekstrelerin ve AgNP'lerin antioksidan aktivitesi, DPPH (2,2-difenil-1-pikrilhidrazil) yöntemi ile belirlenmiştir. Fitosentezlenen nanopartiküllerin antioksidan potansiyele sahip olduğu gözlemlenmiştir. Son olarak, AgNP'ler karbon pasta elektrot (CPE) için modifiye edici malzeme olarak kullanılmış ve yük transfer direnci ve askorbik asit sinyali üzerindeki etkileri elektrokimyasal empedans spektroskopisi (EIS), dönüşümlü voltametri (CV) ve kare dalga voltametrisi (SWV) yöntemleri kullanılarak araştırılmıştır. E1-1/CPE, askorbik asit için iyi elektro-katalitik oksidasyon sağlamıştır ve yeni sensörlerin geliştirilmesi için kullanılabilir. Sonuç olarak, AgNP'lerin yeşil sentezi sürecinde sentez parametreleri, AgNP'lerin sadece boyut ve boyut dağılımını değil, aynı zamanda antioksidan aktivitelerini ve elektrokimyasal özelliklerini de değiştirdikleri için hayati önem taşımaktadır.

Anahtar Kelimeler
Yeşil kimya, gümüş nanopartikül, *Salvia fruticosa* Mill., antioksidan aktivite.

Article History: Received: Dec 23, 2021; Revised: Mar 15, 2022; Accepted: Apr 7, 2022; Available Online: Oct 5, 2022.

DOI: https://doi.org/10.15671/hjbc.1040656

Correspondence to: D. Erkakan, Graduate School of Natural and Applied Sciences, Ankara University, Ankara, Turkey.

E-Mail: damlakumser@gmail.com

INTRODUCTION

In the last decade, green nanotechnology has been introduced as an emphasized area of research. It is an interdisciplinary field that aims to prepare nanomaterials via green methods which follow the green chemistry principles [1]. In modern material science, the synthesis of noble metal nanoparticles such as Au, Ag, Pt, and Pd is an important field of research since they exhibit enhanced physicochemical, biochemical, and optoelectronic characteristics when compared to their bulk counterparts [2, 3]. In particular, silver nanoparticles (AgNPs) have been widely used in products ranging from textile industries to pharmaceutics due to their unique, size and shape depended optical, electrical, thermal properties, as well as antimicrobial, antifungal, and high catalytic activity [2, 4, 5]. Silver nanoparticles are frequently used in areas where there is human contact, such as detergents, socks, and cosmetics. Thus, for the synthesis of nanoparticles, the development of green and eco-friendly methods that do not require hazardous chemicals is today's necessity. [6].

Using biological methods for the synthesis of metal nanoparticles is also a preferable alternative because of its simplicity, sustainability, environmental friendliness, efficiency, and cost-effectiveness as compared to physical or chemical synthesis methods [7]. Among all biological methods, nanoparticle synthesis using plant extract has some preferable aspects such as being able to produce more stable nanoparticles in a shorter synthesis time and being cost-effective [8]. In this work the *Salvia fruticosa* Mill. extract was selected as a reducing and capping agent.

Salvia fruticosa Mill. (synonym, *Salvia triloba* L.f.) which is also known as Anatolian sage belongs to the *Lamiaceae* family and is one of the important sage species which naturally grows throughout the Mediterranean region of Turkey. It is commonly used as herbal tea and to treat diseases like colds, bronchitis, tuberculosis, hemorrhage, aches, epilepsy, and menstrual disorders [9] because of its anti-inflammatory [10], antimicrobial [11], antifungal [12], and antioxidant [13] properties. In research conducted by C. Dincer et al., seventeen different phenolic compounds (7 phenolic acids and 10 flavonoids) have been identified by HPLC analysis in aqueous extract of *Salvia fruticosa* It has been found that rosmarinic, p-coumaric, and caffeic acids are the main phenolic components [14]. *S. fruticosa* also contains essential oils like 1,8-Cineole, camphor α-thujone, β-thujone, and β-caryophyllene [15].

In literature, a tremendous number of research about the synthesis of silver nanoparticles using the extracts of various types of plants has been reported [16]. Considering studies conducted only with plants belonging to the *Salvia* species, reported results are confirmed that extracts of *Salvia officinalis* [17], *Salvia leriifolia* Benth. [7, 18], *Salvia splendens* Sellow ex Roem. & Schult. [19], *Salvia leucantha* Cav. [20], *Salvia microphylla* Kunth [21], *Salvia limbata* C.A. Mey [3,22], *Salvia hispanica* L. [1], *Salvia spinosa* [2], *Salvia sclarea* [23], and *Salvia miltiorrhiza* Bunge [24] had the capability of phytosynthesize AgNPs. There are also specific studies on the effects of green synthesis parameters on silver nanoparticle formation and stability [25,26].

Evaluation of the antioxidant behavior of phytosynthesized AgNPs is useful to determine their potential applications. Therefore, a lot of reports including the antioxidant capacity of silver nanoparticles phytosythesized by plant extracts have been published [27–29]. Some attempts were made to investigate the relation between the phytosythesized AgNPs and their antioxidant capacity. In a study conducted by Priya et al., antioxidant activities of chemically synthesized AgNPs and biosynthesized AgNPs were compared [30]. Akbal and coworkers investigated the antioxidant capacities of seven different leaf extracts and their effects on the formation rates of silver nanoparticles [31]. Bunghez et al. discussed the stabilities and antioxidant properties of nanoparticles synthesized using ornamental plants [28].

However, to the best of our knowledge, the effect of synthesis parameters on the antioxidant activity of phytosynthesized AgNPs has not been reported yet. The current study aims to synthesize silver nanoparticles with the aqueous extract of *Salvia fruticosa* in a greener way and investigate the effects of synthesis parameters on the formation, structure, and antioxidant activity of nanoparticles. In addition, the carbon paste electrodes modified with phytosynthesized silver nanoparticles were successfully fabricated and their electrochemical properties were studied preliminarily by using cyclic voltammetry, square wave voltammetry, and electrochemical impedance spectroscopy techniques.

MATERIALS and METHODS

Chemicals and reagents

Graphite powder and potassium ferrocyanide ($K_4Fe(CN)_6$) were purchased from Merck and Riedel-de Haen. Silver nitrate ($AgNO_3$), ethanol (EtOH), 1,1-Diphenyl-2-picrylhydrazyl (DPPH), potassium chloride (KCl), sodium phosphate dibasic (Na_2HPO_4), sodium phosphate monobasic (NaH_2PO_4), and L-ascorbic acid were purchased from Sigma–Aldrich. Mineral oil was purchased from an oil refinery in the highest purity. Solutions were prepared with ddH_2O. The fresh *Salvia fruticosa* was collected from Kaş, Turkey. The collected plants were shade dried at room temperature for three days. The dried material was stored in a cool and dry place for further usage.

Instrumentation

The UV-visible spectra of AgNPs were obtained on UV–visible spectrophotometer (Varian Cary 50 Bio). Double distilled water was used as a baseline. The samples were measured without further dilution. The spectra were recorded in the wavelength region from 350 to 700 nm. Transmission electron microscopy (TEM) images obtained by FEI Tecnai G2 Spirit BioTwin were used to observe the morphology of nanoparticles. For TEM analysis, samples were dropped on carbon-coated copper grids after being dispersed by sonication. Fourier transform infrared (FTIR) measurements of the extract and AgNPs were carried out on a Thermo Scientific Nicolet iS50 FTIR Spectrometer in the range of 4000–600 cm^{-1}. The pH of the buffer solution was measured with Thermo Scientific Orion Star A211 model digital pH meter. The antioxidant activity analysis was performed using a µQuant microplate spectrophotometer (Biotek). All electrochemical experiments were carried out by using the electrochemical work station CHI-660b model in a conventional three-electrode cell where 3 mm carbon paste electrodes were used as a working electrode while a platinum wire and Ag/AgCl saturated electrode were served as a counter and a reference electrode, respectively.

Preparation of *Salvia fruticosa* Mill. extracts

First of all, *S. fruticosa* leaves were pestle to powder in a mortar. Extracts were prepared at three different concentrations by separately adding 2 g, 5 g, and 10 g of powder to 100 mL of boiled distilled water in a 250 mL beaker and let stand until room temperature approximately 45 minutes. The obtained infusion was filtered with Whatman filter paper no. 1 and denoted as E1, E2, and E3, respectively. The decanted extract was stored in the refrigerator at 4°C and used for the synthesis of the silver nanoparticles. Extract yields were determined by lyophilization of 50 mL of each extract and calculated on a dry basis from equation (1) shown below [32]:

$$\text{Yield } (\%)=(W_1 \times 100)/W_2 \quad (1)$$

Where W_1 was the mass of extract after lyophilization and W_2 was the mass of the dry plant sample.

Synthesis of silver nanoparticles

Synthesis of AgNPs was carried out by adding a various volume of *S. fruticosa* leaf extracts (E1, E2, and E3) into 9 mL of aqueous silver nitrate ($AgNO_3$) solutions and exposing the resulting solution to sunlight. The AgNP formation was observed via color change of the solution from pale yellow to reddish or dark brown and confirmed by UV–Vis spectrophotometry method. All experiments were performed at room temperature. After the completion of the synthesis reaction, dry nanoparticles were obtained by lyophilization for further analysis.

Antioxidant activity

The antioxidant activity of each extract and green synthesized AgNPs was determined by using DPPH (1,1-diphenyl-2-picrylhydrazyl) radical scavenging capacity assay. The method which is used by Arıtuluk et al. was adopted without modification [33]. DPPH (1 mM) radical solution was freshly prepared in ethanol. Samples were prepared at different concentrations by dissolving in ethanol. 50 µL of DPPH radical solution was mixed with 150 µL of different concentrations of samples. The reaction mixture was incubated for 30 minutes in the dark, then absorbance was measured at 517 nm. In this study, since the antioxidant activity of AgNPs was compared with the extract used in their synthesis, a different standard was not required. Radical scavenging activity was expressed as the inhibition percentage and calculated using the following equation (2):

$$\text{Inhibition } \% = [(A_{blank} - A_{sample})/A_{blank}] \times 100 \quad (2)$$

where A_{blank} is the absorbance of the blank (all the reagents except the sample extract) and A_{sample} is the absorbance of the extracts. The assay was carried out in triplicate and the results were expressed as average values. Extract concentration providing 50% inhibition (IC_{50}) was calculated from the plotted graph of inhibition percentage versus the concentrations of the sample.

Preparation of carbon paste electrodes

While preparing the AgNP modified carbon paste electrode (AgNP-CPE), firstly, previously synthesized and lyophilized silver nanoparticles were dispersed in 2 mL of absolute ethanol. Then, the colloidal solution of AgNPs was mixed with 0.5 g graphite powder and dried at room temperature. The AgNP modified carbon paste electrodes were prepared by hand-mixing of AgNP doped graphite powder and silicon oil at a ratio of 70:30 in an agate mortar for 15 minutes. The homogeneous carbon paste was packed into the cavity of a homemade electrode body which was fabricated by cutting the tip of a micropipette (3.0 mm in diameter). A copper wire was connected to the carbon paste to provide the electrical contact. The surface of the electrode was smoothened on a piece of weighing paper. The bare carbon paste electrode (bCPE) was prepared without adding a modifier (silver nanoparticles). Carbon paste electrodes containing different AgNP solutions were labeled as follows: the carbon paste electrodes modified with AgNPs synthesized by mixing 0.3 mM precursor and 0.5 mL of E1, E2, and E3 extracts separately as E1-0.3/CPE, E2-0.3/CPE, and E3-0.3/CPE, respectively. The carbon paste electrodes modified with AgNPs synthesized by mixing 0.5 mL of E1 extract and 0.3mM, 1 mM, and 3 mM precursors were labeled as E1-0.3/CPE, E1-1/CPE, and E1-3/CPE, respectively. Results obtained with AgNPs were compared to the bCPE.

RESULTS and DISCUSSION

Characterization of AgNPs

Transmitting electron microscope (TEM)

Transmitting electron microscope technique was employed to determine the size, shape, and size distribution of AgNPs. The obtained TEM images and particle size distribution histograms of AgNPs synthesized with twelve different reaction solutions containing three different amounts and concentrations of extract into 9 mL of 0.3 mM silver nitrate precursor is shown in Figure 4-7. In TEM images, an amorphous layer that covers the particles is thought to be the stabilizing agent. It was observed that nanoparticles are mostly in a spherical shape with sizes from 2-52 nm. It is known that the morphology of the AgNPs change by the chemical composition of the extracts used for the synthesis [5]. Alike, particle size and size distribution vary depending on the synthesis conditions.

Fourier transform infrared (FTIR)

The possible functional groups of phytochemicals involved in the bioreduction of Ag ions were detected by Fourier transform infrared spectroscopy (FTIR). FTIR spectra of the AgNPs phytosynthesized by mixing 0.5 mL of E1 extract and 9 mL of 0.3 mM silver nitrate precursor are shown in Figure 1.

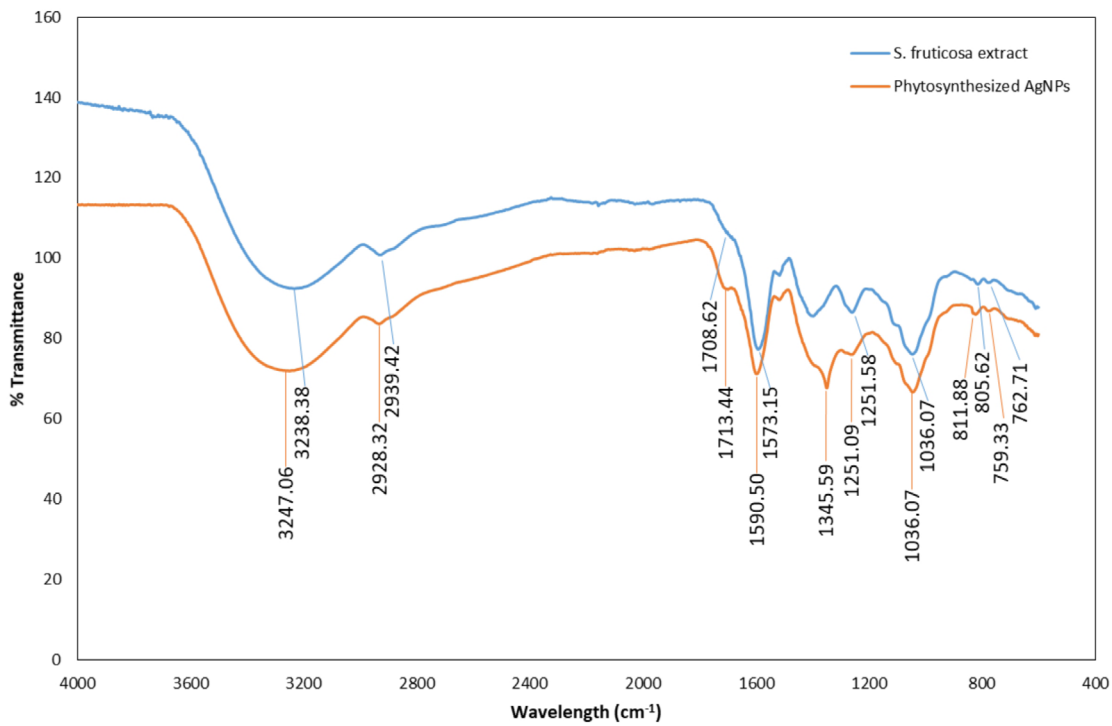

Figure 1. Infrared spectra of *Salvia fruticosa* extract (blue) and phytosynthesized AgNPs (orange).

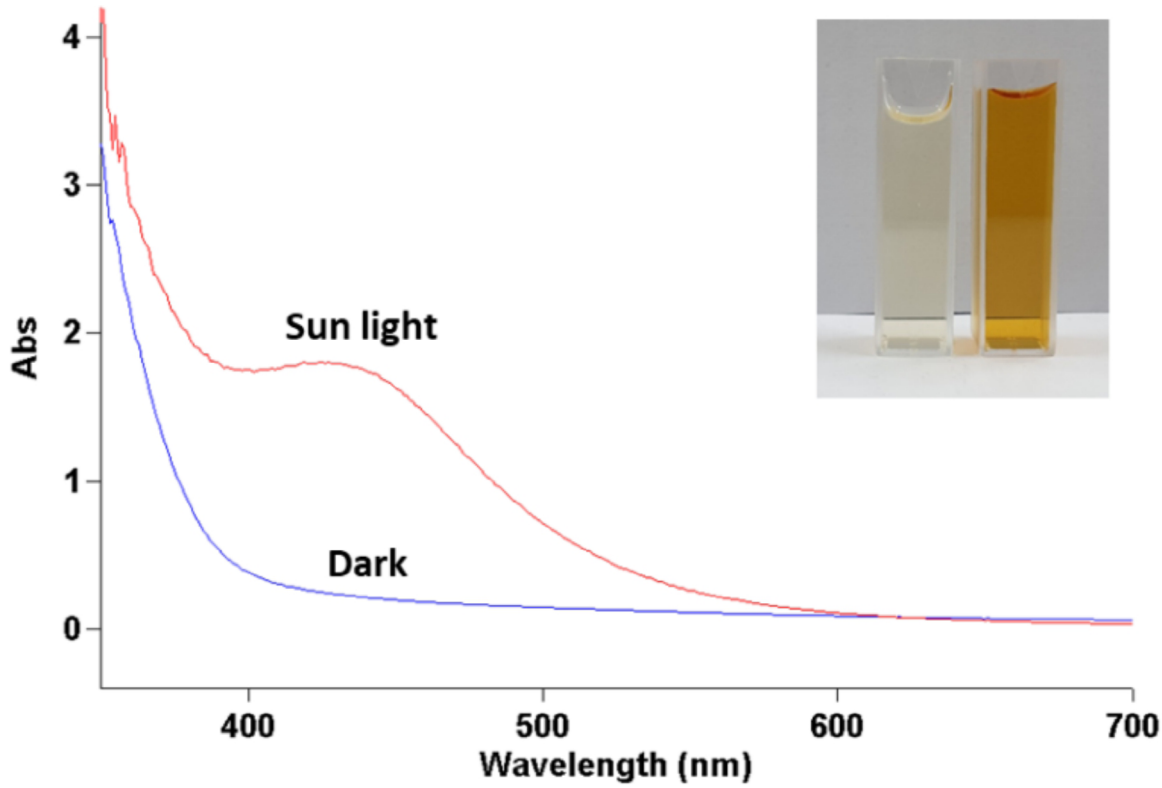

Figure 2. Photograph and UV-visible spectrum of two identical experiments (1 mL of S. fruticosa extract added to 9 mL of 0.3 mM precursor) conducted under different light conditions after 2 h.

Instinct and broad absorption bands at 3247 and 3238 cm^{-1} appear in the presence of intermolecular and intramolecular –OH groups. It indicates abundant flavonoids and phenolic acids, having hydroxyl groups in their structure, in the *S. fruticosa* extract. The bands which appeared at 2928 and 2939 cm^{-1} correspond to aliphatic C–H stretching in lipids [2]. It seems that the bands at 1713 and 1708 cm^{-1} are related to the C = O stretching while the IR bands observed at 1590 and 1573 cm^{-1} could be ascribed to C–C stretching in cyclic alkenes. The major changes in the position of absorption bands between the FTIR spectrum of the *S. fruticosa* extract and phytosynthesized AgNPs were seen at 1411 and 1345 cm^{-1}. These changes can be attributed to the change in vibration of intramolecular –OH groups from stretching to bending. The bands at 1251 and 1036 cm^{-1} could be ascribed to C-O stretching. The bands at 811 and 805 cm^{-1} and also 759 and 762 cm^{-1} represent the presence of C–H in aromatic compounds in the plant extract and the biosynthesized AgNPs. The comparison between the FTIR spectrum of the *S. fruticosa* extract and AgNPs shows that there is a considerable similarity and the involvement of phytochemicals in synthesizing of AgNPs was confirmed with some minor changes in the absorption bands. If so, phytochemicals including OH and CO functional groups have a vital role in reducing and stabilization of AgNPs [2].

Optimization of green synthesis parameters

The effect of different parameters on the synthesis of silver nanoparticles was mostly observed via UV-visible spectroscopy since it is a simple, easy, and effective method. The phytosynthesized silver nanoparticles were characterized by a UV-visible spectrum at the range of 350 to 700 nm. In spectra, the *S. fruticosa* extract presents bands below the wavelength of 350 nm attributed to plant pigments such as flavonoids. The absorption band between 340-620 nm indicates the surface plasmon resonance (SPR) for AgNPs [7]. It is known that the surface plasmon resonance peak depends on the shape and size of silver nanoparticles. Spectrum also changes with the concentration of AgNPs, amount of extract, and the type of phytochemicals present in the extract [34].

Effect of light

The previous researches and preliminary experiments were shown that light is a crucial parameter for the formation of silver nanoparticles for this green synthesis method [35, 36]. Figure 2 shows the spectrum of two identical sets of experiments which one of them let in the dark, the other one keeps under the sunlight for 2 h. As shown in Figure 2, an absorption peak at 435 nm because of the surface plasmon resonance (SPR) of AgNPs has appeared in spectra of solution kept under the sunlight and also the color of the reaction solution changed from pale yellow to orange. However, there was no change in color and spectra of the solution that let stand completely in the dark even 24 hours later. In other words, in the absence of light there is no silver nanoparticle formation. Nevertheless, after exposure of solution kept in dark to the light, formation of silver nanoparticles started within seconds and increased up to 2 hours, after that only slight variation can be observed (Data not shown).

It was reported that *Salvia* species contains abundant flavonoids and phenolic acids [37]. Both phytochemicals are good antioxidants. While phenolic acids are trapping free radicals, flavonoids are free radical scavengers and chelate metals. Moreover, flavonoids are a secondary metabolite and naturally occurring yellow-colored pigments that perform a photo-protective role by absorbing UVA and UVB

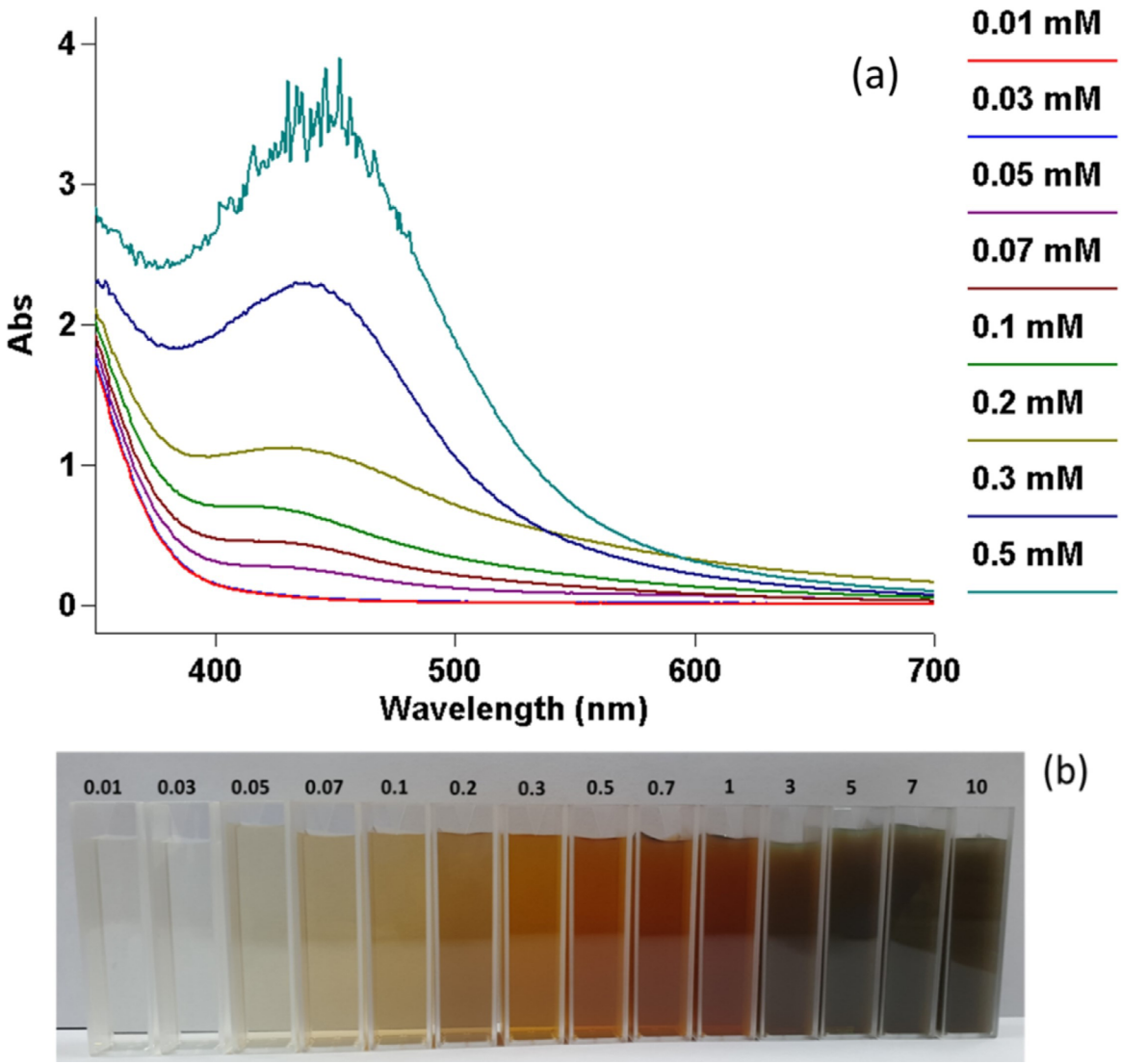

Figure 3. Effect of metal ion concentration in precursor on silver nanoparticle production: (a) UV–Visible spectra and (b) photograph of silver nanoparticle solutions synthesized with 9 mL of AgNO3 at different concentrations and 0.5 mL Salvia extract (E1) incubated for 24 h.

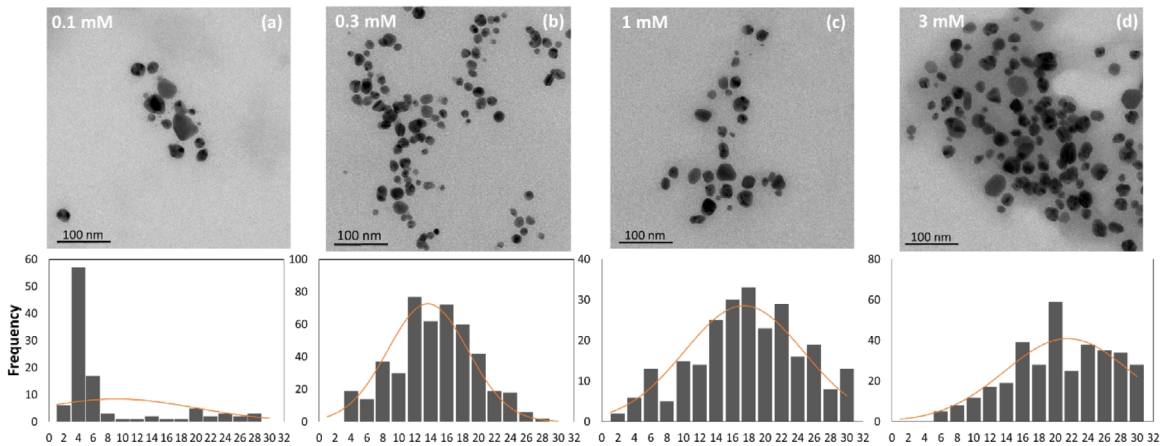

Figure 4. Particle size distribution histograms of AgNPs synthesized by (a) 0.1 mM, (b) 0.3 mM, (c) 1 mM and (d) 3 mM metal ion concentration in precursor.

radiation in plants [38,39]. Therefore, it is supposed that the role of light is providing the production of hydrated electrons by polyhydroxy groups of flavonoids that result in the reduction of Ag^{+} ions to Ag^{0} [40,41].

Effect of metal ion concentration in precursor

To investigate the role of silver nitrate concentration on the silver nanoparticles formation, fourteen precursors with different concentrations were prepared and used to synthesize silver nanoparticles by keeping the extract volume (E1) constant at 0.5 mL. Figure 3 displays the photograph and UV-vis spectra of phytosynthesized AgNPs at different concentrations incubated for 24 h.

From photograph in Figure 3(b), it was observed that the color of the reaction solution changed from colorless to dark brown with an increase in silver ion concentration. As can be seen from Figure 3(a), as the concentration of silver nitrate increased from 0.01 mM to 0.5 mM, the intensity of absorbance band was also increased which indicates the increased concentration of AgNPs. There is no considerable nanoparticle formation till metal ion concentration reached 0.3 mM. At higher concentrations, the noise emerges on the absorbance bands which may be due to exhaustion of capping agent and be caused by the transmission problem at further concentrations. In addition, the location of the SPR peak is shifted toward a higher wavelength. It has been reported that an increase in size and dispersity in AgNPs causes the red shift in the UV-vis spectrum [42]. The increase in particle size and size distribution can also be observed from histograms given in Figure 4.

Moreover, the absorbance bands belonging to the reaction solutions which have higher concentrations than 1 mM are broad and have an absorption tail. This indicates that these reaction solutions contain a large number of large-sized nanoparticles which have size distribution as well. Identical experiments were conducted by only changing extract type (E2 and E3) (Data not shown). All the obtained results were evaluated and 0.3 mM of silver nitrate solution was adopted as a precursor for further experiments since the resulted AgNPs are stable and have narrow size distribution.

Effect of the amount of extract and extract concentration

Yields of extracts (E1, E2, and E3) are calculated as 10.47%, 9.59%, and 9.87% from equation (1), respectively. As expected, it shows that increased dry plant gives more concentrated extract. The effect of extract concentration was investigated by adding three different extracts (E1, E2, and E3) to 9 mL precursors at a constant amount and incubating at room temperature for 24 h. To determine the amount of extract that gives the maximum number of stable AgNPs, three different extracts (E1, E2, and E3) in three different amounts varied from 0.1, 0.5, and 1 mL in 9 mL of 0.3 mM aqueous $AgNO_3$ solution (Figure 5-7).

Figure 5(a) shows UV-vis spectra of AgNPs phytosynthesized varying the volume of E1 after 240 min incubation. It found that increasing the amount of plant extract (E1) from 0.1 to 0.5 mL results in a remarkable increase in the absorption band, attributing to the increase of AgNPs concentration. However, as the plant extract was increased to 1 mL not only did the intensity of absorption band slightly decrease but also the plasmon absorption maximum shifted to shorter wavelengths.

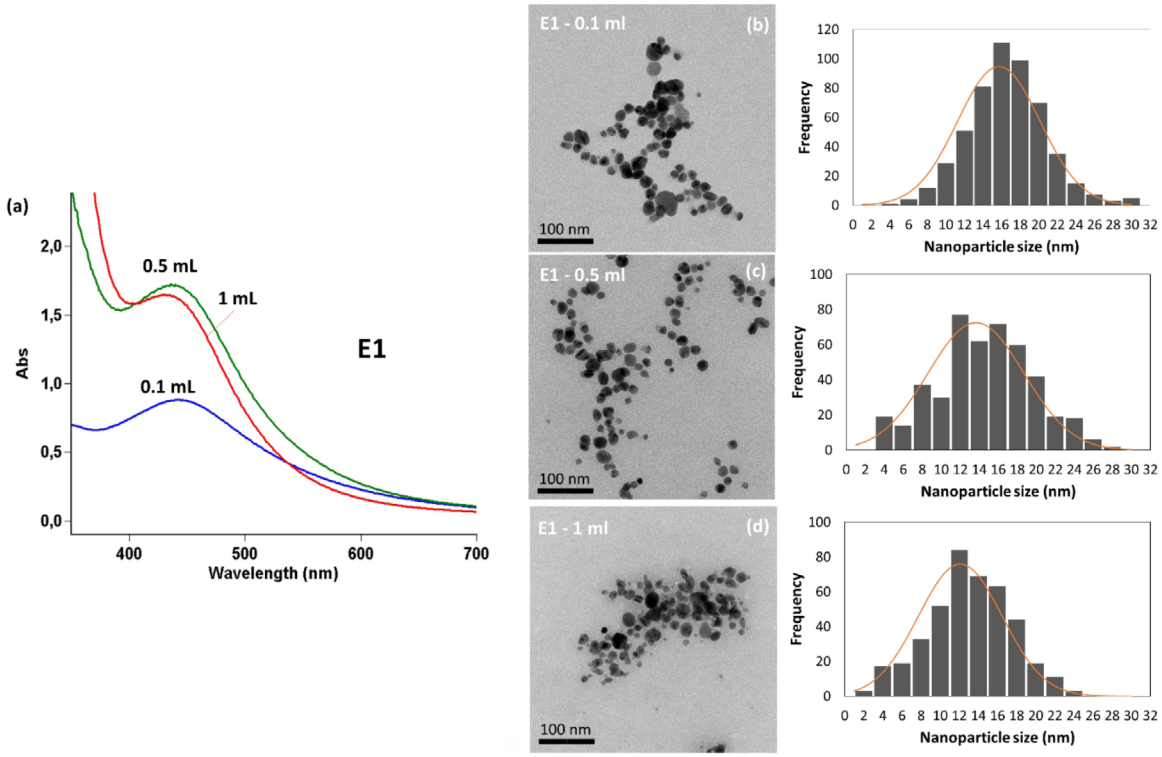

Figure 5. (a) UV-vis spectra (b-d) TEM images and histograms of AgNPs synthesized by adding three different amount (0.1, 0.5, and 1 mL) of E1 extract into 9 mL of 0.3 mM silver nitrate precursor.

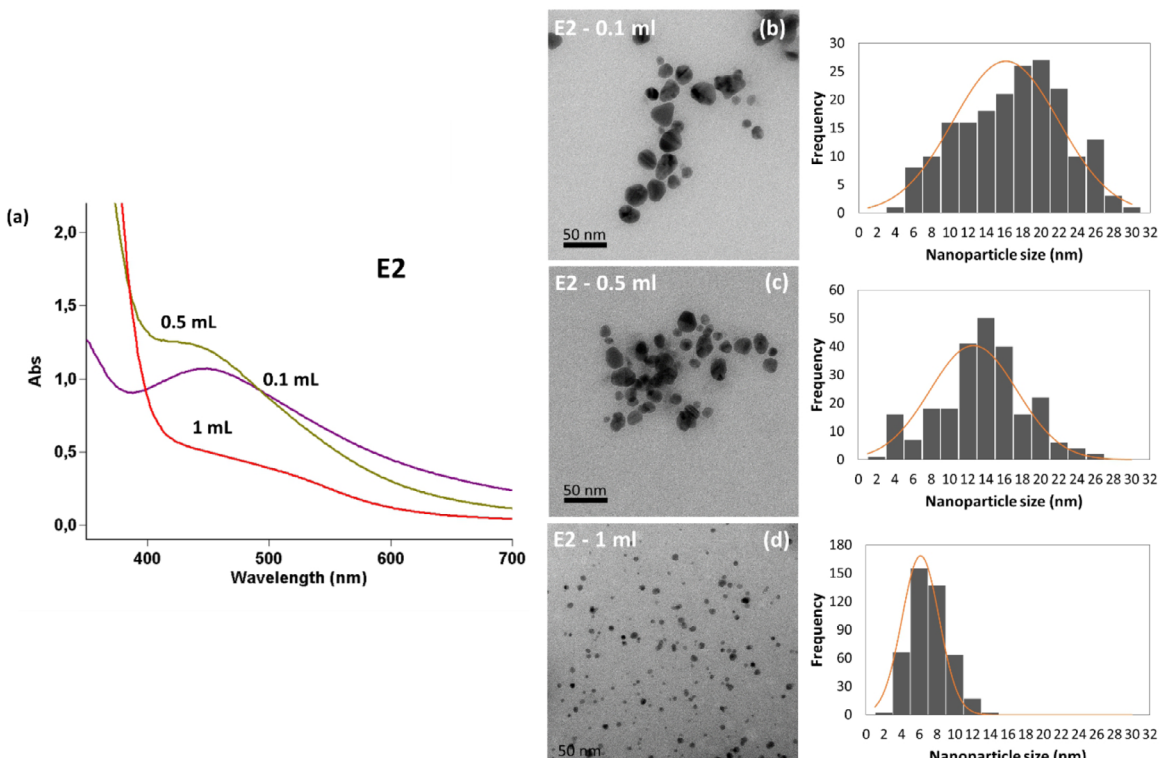

Figure 6. (a) UV-vis spectra (b-d) TEM images and histograms of AgNPs synthesized by adding three different amount (0.1, 0.5, and 1 mL) of E2 extract into 9 mL of 0.3 mM silver nitrate precursor.

This blue shift is indicating the particle size reduction. It was due that the increase in extract amount leads to a faster reduction of silver ions and a larger number of nuclei formation simultaneously and consequently the formation of small AgNPs.

Figure 6(a) shows UV-vis spectra of AgNPs phytosynthesized varying the volume of E2 after 240 min incubation. It illustrates that increasing the amount of plant extract (E2) from 0.1 to 0.5 mL results in only a moderate increase in the absorption band and a decrease in the bandwidth to be considered as less size distribution in larger particles. Results are also supported by histograms of TEM images given in Figure 6(b-d). The absorption band observed at higher wavelengths than 400 nm ascribed to nanoparticles that have smaller sizes than 10 nm. When the plant extract quantity was increased to 1 mL, a large number of small AgNPs formed. Therefore, it was observed that the plasmon absorption maximum of AgNPs has shifted to higher wavelengths than 400 nm due to the drastic decrease in the size and dispersity of AgNPs.

In Figure 7(a), the formation of AgNPs mostly smaller than 10 nm was encountered in the amount of 0.5 mL of E3 extract. It was similar to the result obtained by 1 mL of E2 extract but not exactly the same. This may be explained by the change in the physicochemical conditions with the presence of the greater amount of phytochemicals in the reaction solution (e.g., agglomeration, super-saturation, the effect of secondary interactions, etc.) [43].

The effect of extract concentration can be examined from Figure 8(a-c). As it can be seen from Figure 8(a), at a lower extract amount, a decrease in the extract concentration causes a gradual decrease in the absorbance with a slight blue shift in plasmon absorption maximum. Blue shift means a small decrease in particle size. In Figure 8(b), an increase in the extract concentration leads to a considerable decrease in the absorbance intensity and formation of nanoparticles mostly smaller than 10 nm. In other words, at a lower extract amount, the variation of extract concentration affects the number of nanoparticle**s** formed but its morphology and size distribution stays similar. On the other hand, at a higher extract amount, the same variation in extract concentration has a considerable effect on both the size, morphology, and size distribution of nanoparticles.

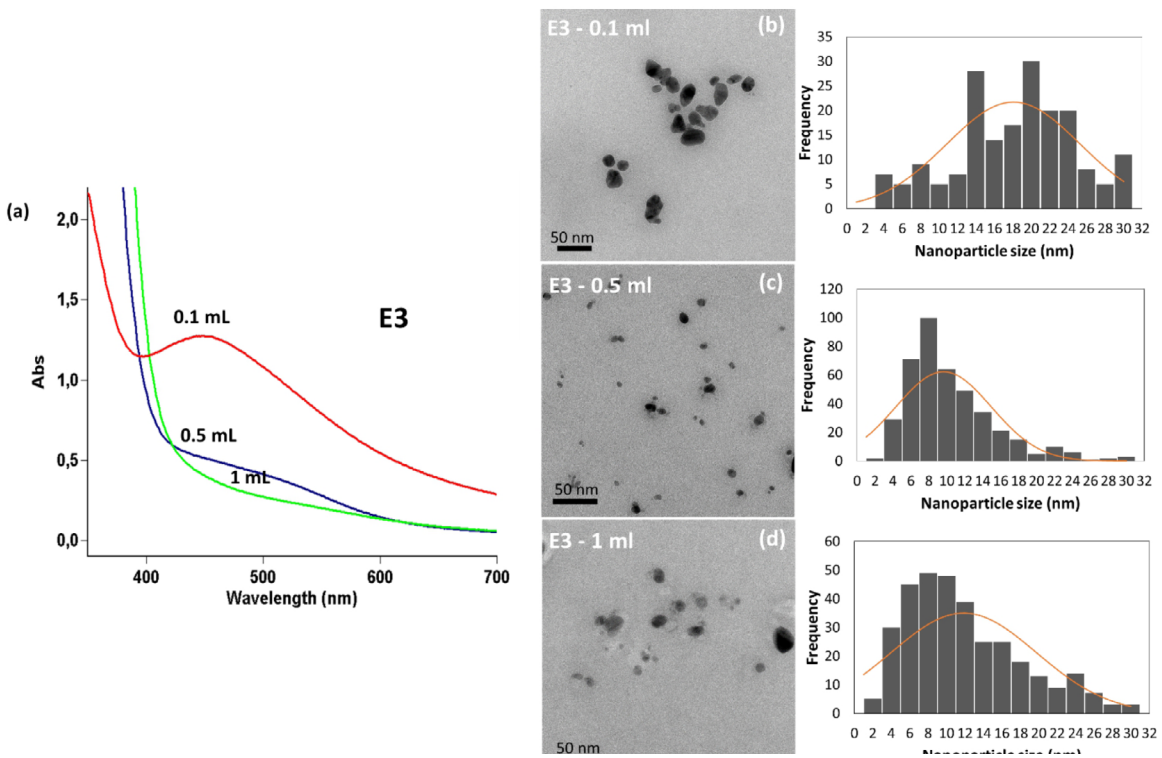

Figure 7. (a) UV-vis spectra (b-d) TEM images and histograms of AgNPs synthesized by adding three different amount (0.1, 0.5, and 1 mL) of E3 extract into 9 mL of 0.3 mM silver nitrate precursor.

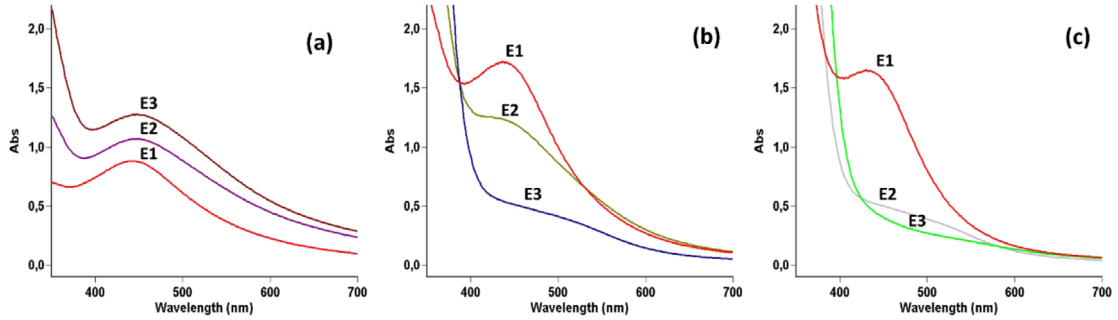

Figure 8. UV-vis spectra of AgNPs synthesized by adding (a) 0.1 mL (b) 0.5 mL and (c) 1 mL of each extract (E1, E2, and E3) into 9 mL of 0.3 mM silver nitrate precursor.

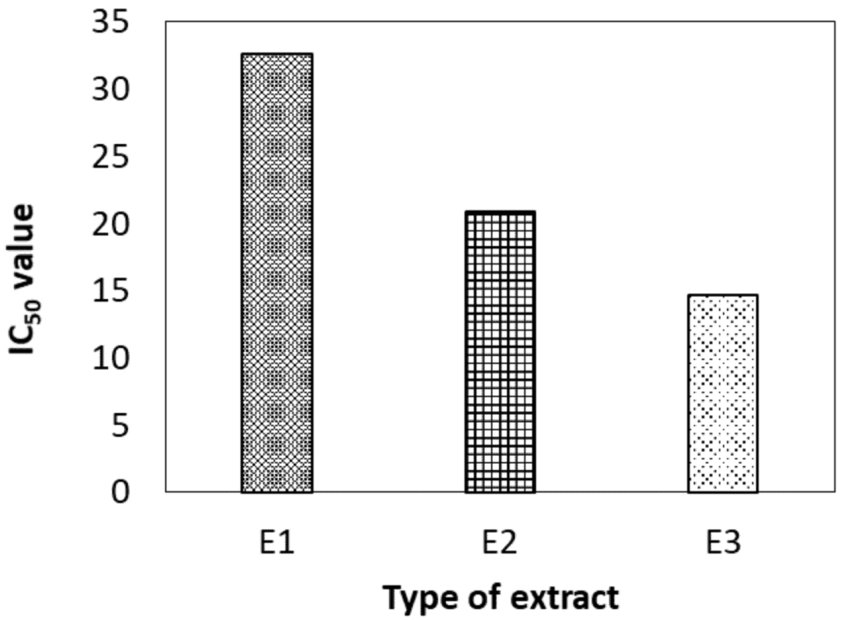

Figure 9. IC_{50} values of three different *S. fruticosa* extracts (E1, E2, and E3).

As a result of these, the slightest variation in high extract concentrations (E3) has a huge effect on nanoparticle formation. On the other hand, low extract concentrations (E1) provide more opportunities for nanoparticle production optimization.

DPPH assay for antioxidant activity

The antioxidant activity of phytosynthesized AgNPs and three different aqueous extracts of *S. fruticosa* was evaluated by DPPH radical scavenging assay. DPPH (1,1-diphenyl-2-picrylhydrazyl) is a stable free radical compound and has the ability to accept electrons from antioxidant compounds or silver nanoparticles. In antioxidant activity assays, a compound known to have good antioxidant (radical scavenging) properties are usually chosen as the standard. In this study, a different standard was not required since the antioxidant activity of AgNPs was compared with the extract used in their synthesis. The antioxidant activity of the extracts is given as IC_{50} values in Figure 9.

The antioxidant amount that is required to halve the initial DPPH concentration is called IC_{50}. The lower the IC_{50} value of a compound means that the higher antioxidant activity it has. In other words, the IC_{50} value of a compound is inversely proportional to its antioxidant activity [44]. Accordingly, as can be seen in Figure 9, E3 extract

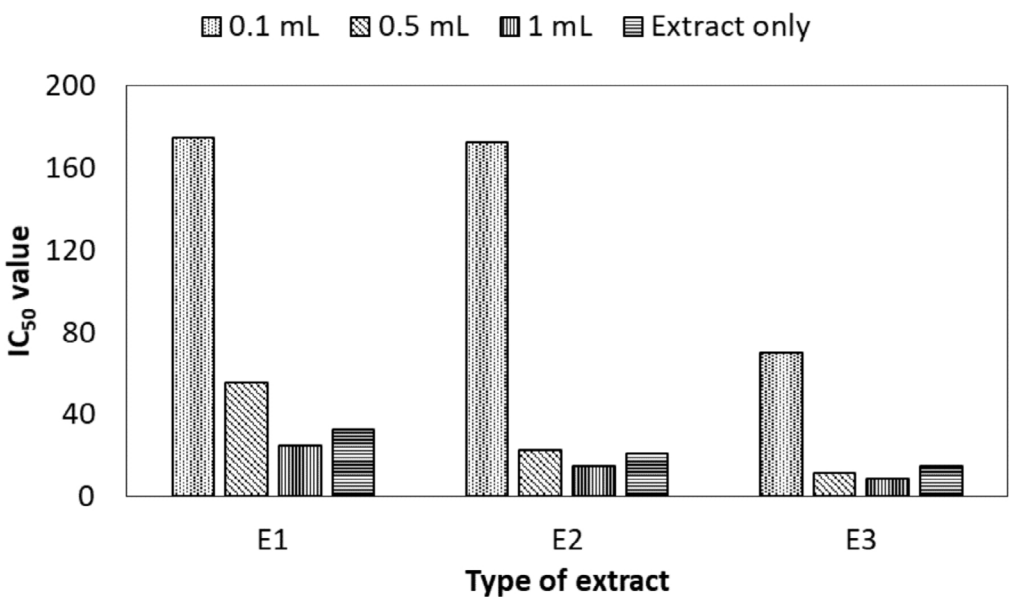

Figure 10. IC_{50} values of extracts only (E1, E2, and E3) and AgNPs phytosynthesized by mixing 0.3 mM AgNO3 and different amounts (0.1, 0.5, and 1 mL) of S. fruticosa extracts.

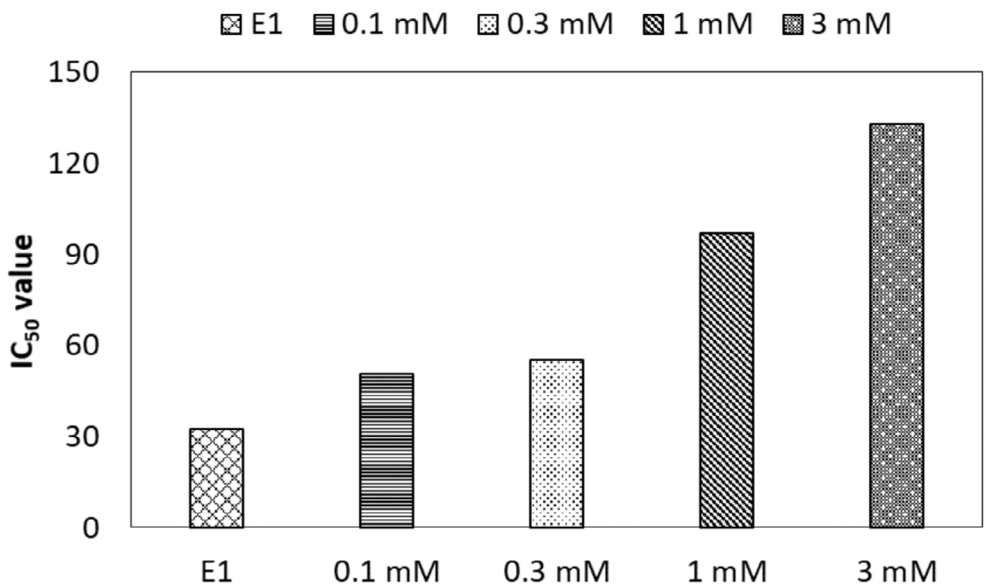

Figure 11. IC_{50} values of S. fruticosa extracts (E1) only and AgNPs phytosynthesized by mixing 0.5 mL of E1 and four different concentrations of metal ion precursor, separately.

has the lowest IC_{50} value which also means that it has the highest antioxidant activity. Considering that the extract yield is ~10% for all three extracts, the increase in the weight of dry matter used in extract preparation results in a higher amount of dissolved substances with antioxidant properties in the extract, which explains the increase in antioxidant activity.

In this study, antioxidant activity assay was performed for 12 different AgNP solutions which have different synthesis parameters. Three different types of *S. fruticosa* extract which have different concentrations were used and the antioxidant activity increased with increasing both concentration and amount of extract. The finding reveals that the phytosynthesized AgNPs pos-

sessed free radical scavenging activity that changes depending on the synthesis parameters. As it can be seen from Figure 10, a significant shift in the DPPH radical scavenging ability was observed according to extract amount.

AgNPs synthesized with 0.1 mL of the extract have the lowest DPPH radical scavenging activity. The result for AgNPs synthesized with 1 mL of extract exhibited a higher DPPH radical scavenging activity when compared to the aqueous *S. fruticosa* extract used in its phytosynthesis although the extract was diluted by 10:1 in the precursor. Thus, it can be simply said that nanoparticles also have antioxidant activity. Nevertheless, the antioxidant capacity of the silver nanoparticles was dependent on not only the amount but also the concentration of extract used in the synthesis.

The antioxidant activity of the silver nanoparticles phytosynthesized with different metal ion concentrations is given as IC_{50} values in Figure 11.

In the synthesis mixture, when extract concentration and amount were kept constant and metal ion concentration is increased, the scavenging ability decreased in a metal ion concentration-dependent manner. The antioxidant activity decreased despite the increasing concentrations of AgNPs. Although there is an increase in the number of nanoparticles formed when 0.5 mL of E1 extract is added into 0.1 mM and 0.3 mM metal ion solutions, there is no significant change in antioxidant activity. In this case, it can be estimated that only some part of the extract is involved in the formation of nanoparticles, but there is still an amount of excess extract which have antioxidant activity in the medium. It can also be estimated that the antioxidant activity is closely related to the amount of extract left in the medium. Moreover, it can be assumed that when the metal ion concentration is increased further by keeping the amount of added extract constant, there is a decrease in the amount of extract -having antioxidant activity- remaining in the reaction medium, and accordingly, there is a decrease in antioxidant activity. It can be concluded that antioxidant activity is not only caused by silver nanoparticles. In the presence of silver nanoparticles, an increase in antioxidant activity can be attributed to the that nanoparticles are in a synergistic effect with the extract and contribute to antioxidant activity by facilitating electron transfer.

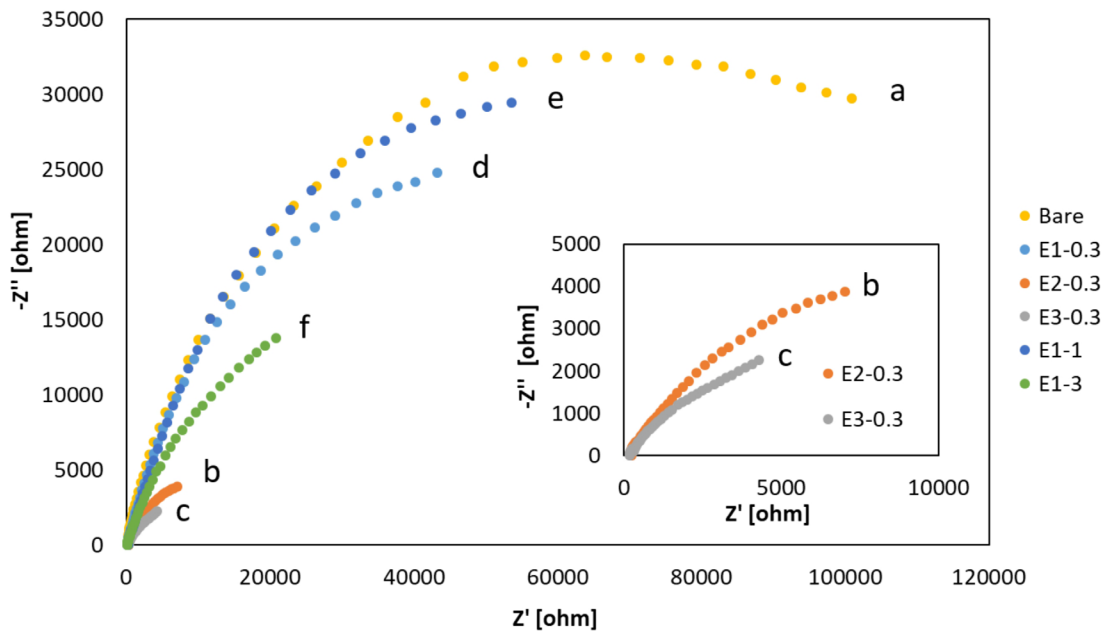

Figure 12. Nyquist diagrams of (a) bare CPE, (b) E1-0.3/CPE, (c) E2-0.3/CPE, (d) E3-0.3/CPE, (e) E1-1/CPE, and (f) E1-3/CPE in 0.3 mol/L KCl solution containing 1.0 mmol/L $Fe(CN)6^{-4/-3}$ in open circuit mode, with a frequency range of 0.1 to 100,000 Hz and amplitude of 5 mV.

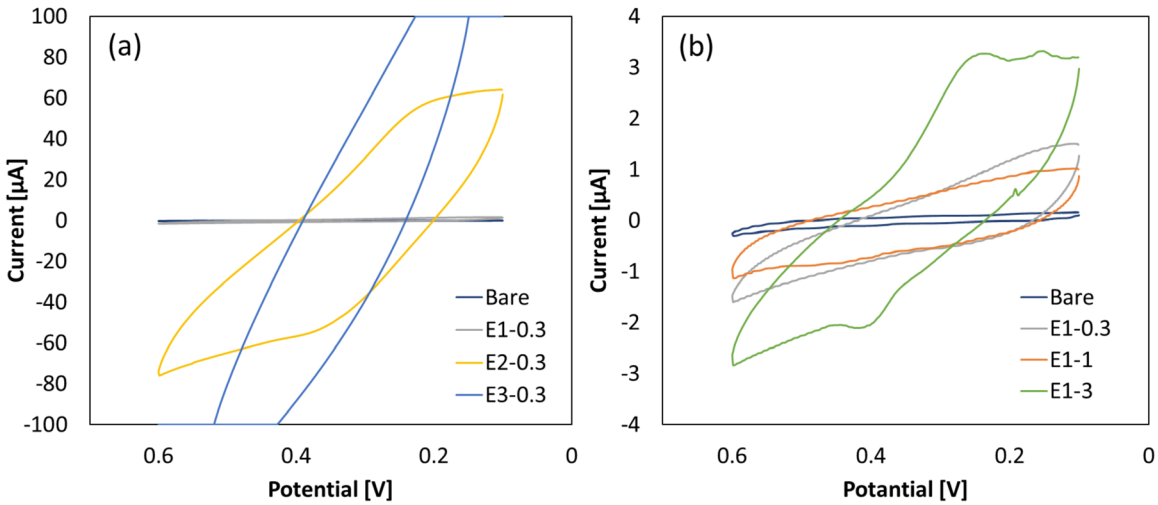

Figure 13. Cyclic voltammograms of bCPE and CPEs modified with AgNP synthesized via (a) different extract concentrations and (b) different precursor concentrations in 0.1 M phosphate buffer solution at pH 7 at a scan rate of 50 mVs^{-1} (n=5).

Electrochemical impedance spectroscopy

Electrochemical impedance spectroscopy (EIS) was used to determine the charge transfer resistance (R_{ct}) of each modified carbon paste electrode. Thus, the differentiation depending on the nanoparticles in the carbon paste matrix was evaluated. Figure 12 shows the impedance spectra obtained by bare CPE and AgNP modified CPE in 0.3 mol/L KCl solution containing 1 mmol/L $K_4[Fe(CN)_6]$.

It is known that the diameter of the semicircle, which corresponds to the charge-transfer limited process, represents the charge-transfer resistance at the electrode surface [45]. The results show that the obtained R_{ct} values were: bare CPE (R_{ct} ≈ 131.4 kΩ), E1-0.3/CPE (R_{ct} ≈ 83.5 kΩ), E2-0.3/CPE (R_{ct} ≈ 24.2 kΩ), E3-0.3/CPE (R_{ct} ≈ 13.6 kΩ), E1-1/CPE (R_{ct} ≈ 104 kΩ), and E1-3/CPE (R_{ct} ≈ 66 kΩ). As it can also be seen from the Nyquist diagram, when compared to the bare CPE, there was a reduction in the electrical resistance after the modification of CPE with different colloidal silver solutions, which may be attributed to both the antioxidant activity of extract and the conductive capacity of AgNPs.

There was a drastic decrease in the R_{ct} values when carbon paste electrodes modified with E1-0.3, E2-0.3, and E3-0.3 solutions are compared with each other. As previously mentioned, in addition to silver nanoparticles, there is also excess extract in the modification solutions prepared with 0.3 mM silver nitrate precursor. This indicates that the electronic charge transfer process is facilitated with increased extract concentration, assuming the same amount of colloidal silver in modification solutions.

The comparison of R_{ct} values obtained by carbon paste electrodes modified with E1-0.3, E1-1, and E1-3 solutions showed that there is an increase at the R_{ct} value despite an increase in silver nanoparticles in the carbon paste matrix. This result is not only due to the increase in the number of silver nanoparticles but also due to the decrease in the amount of extract in the modification solution. Again as mentioned before, there is also no or a little amount of excess extract in the modification solutions prepared with 1 mM silver nitrate precursor. This means that the facilitation of electron transfer resulting from the extract is reduced. However, when compared to bare CPE, the electrical conductivity of E1-1/CPE was enhanced owing to an increase in silver nanoparticle amount in the carbon paste matrix. There is a noticeable decrease in charge transfer resistance of E1-3/CPE which is attributed only to the further increase in silver nanoparticle amount in the carbon paste matrix. It has been a verification that the addition of silver nanoparticles had provided faster electron transfer.

Ascorbic acid determination

AgNPs, as conductive nanoparticles were used for modification of CPE and cyclic voltammetry, were used to study the electro-activity of modified carbon paste electrodes. Before starting the voltammetric experiments, the working electrode is standardized with an open circuit potential in the appropriate buffer solution until the current values are constant [46]. Figure 13 shows the electrochemical responses (current vs. potential) of bare CPE and AgNP modified CPE in 0.1 M phosphate buffer solution (pH 7).

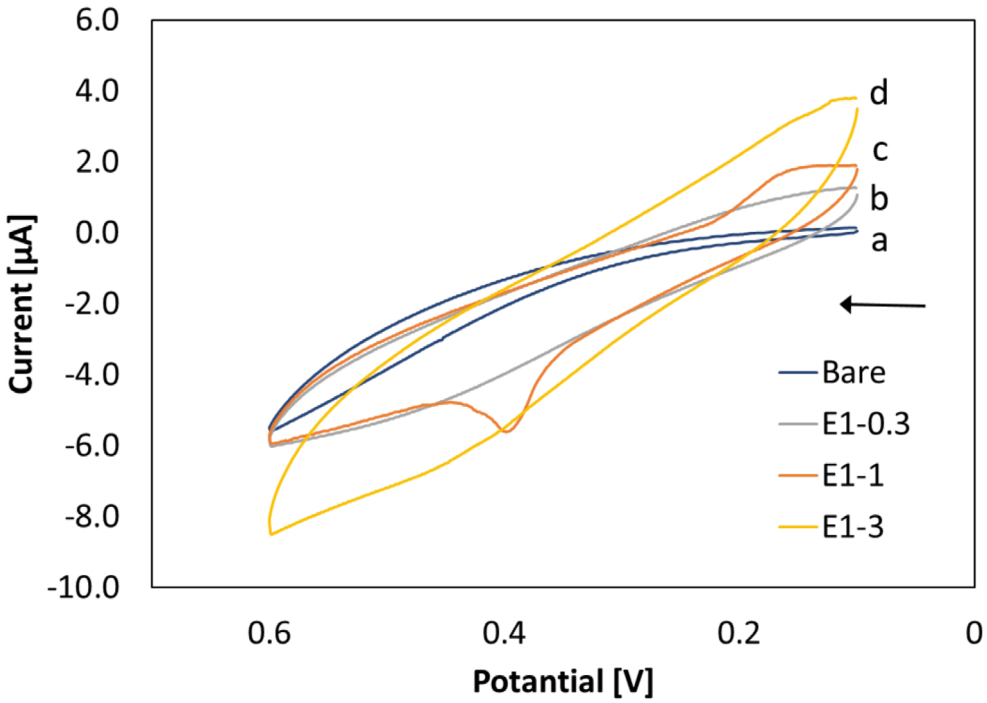

Figure 14. Cyclic voltammograms of (a) bare CPE, (b) E1-0.3/CPE, (c) E1-1/CPE, and (d) E1-3/CPE with the presence of 500 µM ascorbic acid in 0.1 M.

EIS data shows that the charge transfer resistances of the carbon paste electrodes modified with AgNPs synthesized with E2 and E3 extracts (E2-0.3/CPE and E3-0.3/CPE) are lower compared to bCPE. Because of this, as can be seen from Figure 13, a very high current flows through the electrode surface in the small potential range. This limits the use of these electrodes in applications. Therefore, only the electrodes modified with nanoparticles synthesized using E1 were used in further studies. Carbon paste electrodes modified with AgNPs synthesized by adding the same amount of extract (0.5 mL of E1) into different concentrations of precursor (0.3 mM, 1 mM, and 3 mM) were prepared (E1-0.3/CPE, E1-1/CPE, and E1-3/CPE) and utilized to determine ascorbic acid.

The electro-catalytic reduction of ascorbic acid was preliminarily studied with CV in order to examine the performances of bCPE, E1-0.3/CPE, E1-1/CPE, and E1-3/CPE. CVs obtained in the presence of AA in 0.1 M PB solution (pH = 7) at a scan rate of 50 mV/s are shown in Figure 14.

While bCPE has not responded to the analyte AA, E1-1/CPE exhibited a redox peak located at about 0.4 V (vs. Ag/AgCl) for ascorbic acid. Although the voltammograms of E1-0.3/CPE and E1-1/CPE are quite similar, determination of ascorbic acid becomes possible owing to increased nanoparticle amount in the carbon paste matrix. Nevertheless, further increase in the number of nanoparticles in the carbon paste matrix caused deterioration in the electrode performance. Thus, it can be said that the AgNPs phyosynthesized with certain synthesis conditions exhibited a catalytic activity toward the oxidation of ascorbic acid.

The voltammograms at increasing concentrations of AA are given in Figure 15. As can be seen in Figure 15, in the absence of AA, no distinctive peak is observed, while the addition of AA results in an anodic peak that increases in proportion to the AA concentration.

Figure 16 show that the plot of peak current versus ascorbic acid concentration is linear for two different concentration ranges (5-250 µM and 250-750 µM) of ascorbic acid, with the equation being $I_p(\mu A) = -0.0005C_{AA} - 0.3642$ ($R^2 = 0.9988$) and $I_p(\mu A) = -0.0047C_{AA} + 0.6634$ ($R^2 = 0.9984$), respectively, where C_{AA} is the micromolar concentration of ascorbic acid and I_p is the peak current. In the present work, the maximum anodic peak current was obtained at 750 µM for ascorbic acid by cyclic voltammetry.

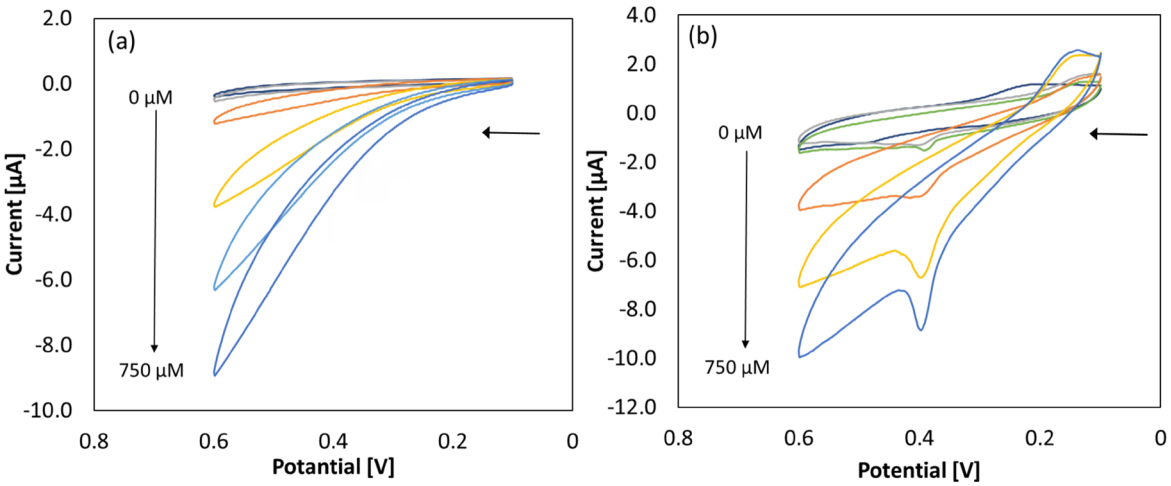

Figure 15. Cyclic voltammograms of (a) bare CPE and (b) E1-1/CPE in 0.1 M phosphate buffer solution, pH 7, with ascorbic acid concentrations of 0, 5, 50, 250, 500 and 750 µM at a scan rate of 50 mVs–1. Arrow corresponds to the direction of forward scan as oxidation, and reverse scan as reduction.

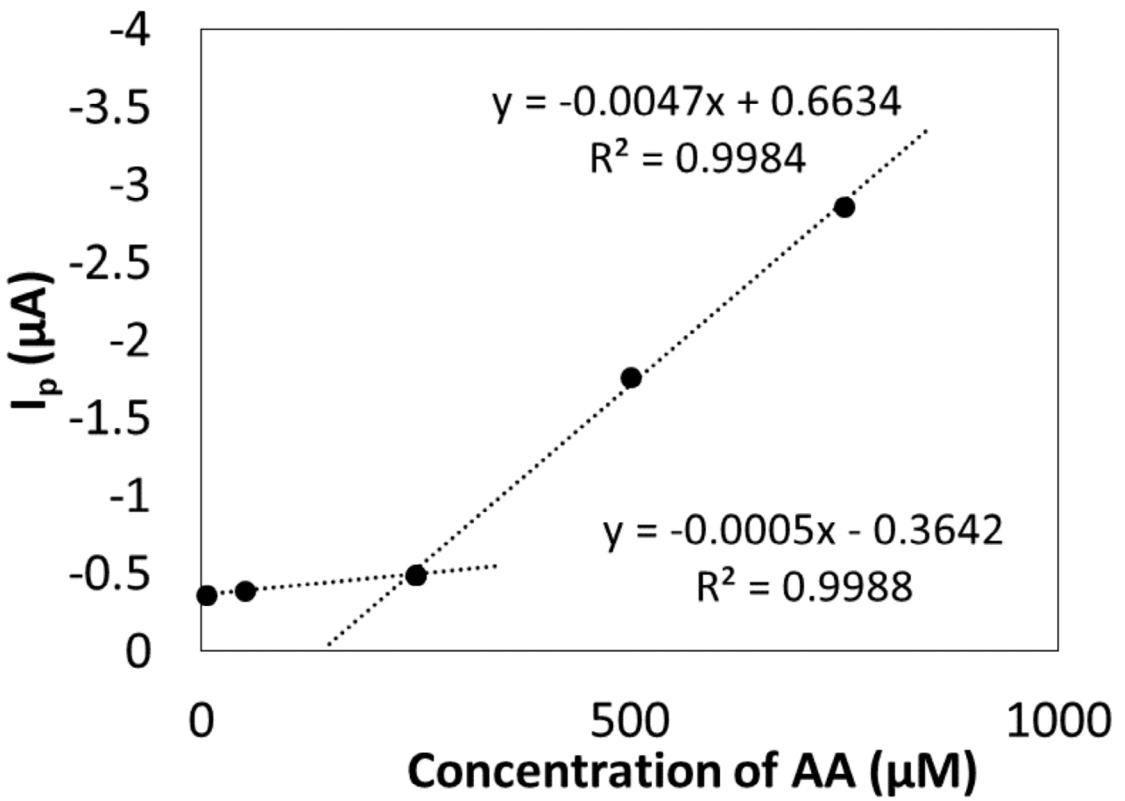

Figure 16. The plot of peak current versus ascorbic acid concentration.

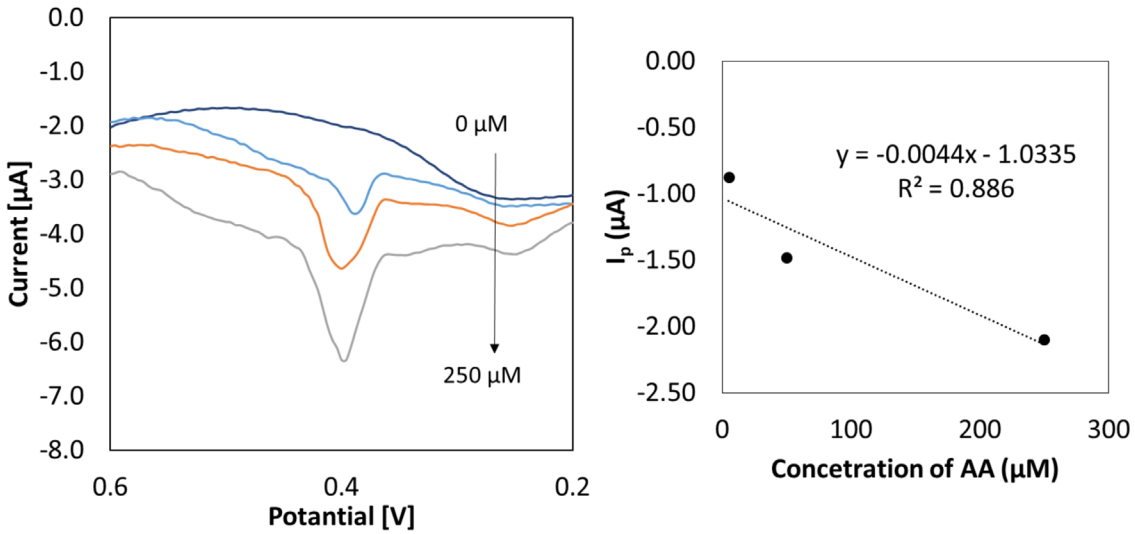

Figure 17. Square wave voltammogram of E1-1/CPE in 0.1 M phosphate buffer solution, pH 7, with ascorbic acid concentrations of 0, 5, 50, and 250 µM at a scan rate of 50 mVs^{-1}.

It is also possible to determine ascorbic acid with the square wave voltammetry (SWV) method in the range of 5-250 µM. Figure 17 shows the plot of peak current versus ascorbic acid concentration with the equation being $I_p(\mu A)=-0.0044C_{AA}-1.0335$ ($R^2=0.8860$) and its voltammogram as inset. At higher concentrations, the distinctive ascorbic acid peak is masked by other current signals and it is not possible to detect ascorbic acid. The maximum anodic peak current was obtained at 250 µM for ascorbic acid by square wave voltammetry. By using E1-1/CPE as a working electrode, ascorbic acid was determined by both SWV and CV. According to the results, E1-1/CPE can be utilized for the development of new sensors.

CONCLUSION

In the present study, stable colloidal silver nanoparticles were synthesized with the phytochemicals present in the aqueous extract of *Salvia fruticosa*. The phytosynthesis of AgNPs is a photo-induced reaction. The effect of synthesis parameters was studied and it has been observed that an increase in extract amount causes a decrease in particle size of AgNPs. Moreover, the change in extract concentration has more effect on resultant nanoparticle morphology. Consequently, these results confirmed that the amount of extract, extract concentration, and metal ion concentration in precursors has an important effect on controlling not only the size and size distribution of the AgNPs but also their stability. The optimum reaction mixture was determined as 9 mL of 0.3 mM silver nitrate solution and 0.5 mL of *S. fruticosa* Mill. extract having 20 g/L concentration (E1). AgNPs synthesized with the optimum reaction mixture were stable in aqueous formation for more than six months. According to DPPH radical scavenging assay results, it was proved that AgNPs have notable antioxidant activity. Also, it was suggested that nanoparticles are in a synergistic effect with the extract and contribute a lot to the antioxidant activity. Finally, the silver nanoparticles modified carbon paste electrodes were successfully fabricated and their electrochemical properties were studied. The EIS results show the addition of silver nanoparticles into the carbon paste matrix provides faster electron transfer. E1-1/CPE showed good electro-catalytic oxidation of ascorbic acid and ascorbic acid was determined by SWV and CV at concentration ranges (5-250 µM and 250-750 µM). Based on its electrochemical response of ascorbic acid, E1-1/CPE can be utilized for the development of the sensor. Consequently, since the extract is also present in the colloidal solution, the extract itself should be considered as a parameter in new materials where the colloidal solution is used in their production.

Acknowledgments
Authors would like acknowledge the funding from Ankara University Scientific Research Projects Coordination Unit (21L0430016) for conducting this research.

References

1. L. Hernández-Morales, H. Espinoza-Gómez, L.Z. Flores-López, E.L. Sotelo-Barrera, A. Núñez-Rivera et al., Study of the green synthesis of silver nanoparticles using a natural extract of dark or white *Salvia hispanica* L. seeds and their antibacterial application, Appl. Surf. Sci., 489 (2019) 952–961.
2. S. Pirtarighat, M. Ghannadnia, S. Baghshahi, Green synthesis of silver nanoparticles using the plant extract of *Salvia spinosa* grown in vitro and their antibacterial activity assessment, J. Nanostructure Chem., 9 (2019) 1–9.
3. F. Nematollahi, Silver nanoparticles green synthesis using aqueous extract of *Salvia limbata* C.A. Mey, Int. J. Biosci., 6 (2015) 30–35.
4. B. Ajitha, Y.A.K. Reddy, H.J. Jeon, C.W. Ahn, Synthesis of silver nanoparticles in an eco-friendly way using *Phyllanthus amarus* leaf extract: Antimicrobial and catalytic activity, Adv. Powder Technol., 29 (2018) 86–93.
5. D. Arumai Selvan, D. Mahendiran, R. Senthil Kumar, A. Kalilur Rahiman, Garlic, green tea and turmeric extracts-mediated green synthesis of silver nanoparticles: Phytochemical, antioxidant and in vitro cytotoxicity studies, J. Photochem. Photobiol. B Biol., 180 (2018) 243–252.
6. A.U. Khan, Y. Wei, Z.U.H Khan, K. Tahir, S.U. Khan et al., Electrochemical and antioxidant properties of biogenic silver nanoparticles, Int. J. Electrochem. Sci., 10 (2015) 7905–7916.
7. M. Baghayeri, B. Mahdavi, Z. Hosseinpor-Mohsen Abadi, S. Farhadi, Green synthesis of silver nanoparticles using water extract of *Salvia leriifolia* : Antibacterial studies and applications as catalysts in the electrochemical detection of nitrite, Appl. Organomet. Chem., 32 (2018) 1–9.
8. M. Guo, W. Li, F. Yang, H. Liu, Controllable biosynthesis of gold nanoparticles from a *Eucommia ulmoides* bark aqueous extract, Spectrochim. Acta Part A Mol. Biomol. Spectrosc., 142 (2015) 73–79.
9. F.S. Şenol, I. Orhan, F. Celep, A. Kahraman, M. Doğan et al., Survey of 55 Turkish *Salvia* taxa for their acetylcholinesterase inhibitory and antioxidant activities, Food Chem., 120 (2010) 34–43.
10. N.H. El-Sayed, W. El-Eraky, M.T. Ibrahim, T.J. Mabry, Antiinflammatory and ulcerogenic activities of *Salvia triloba* extracts, Fitoterapia, 77 (2006) 333–335.
11. A.P. Longaray Delamare, I.T. Moschen-Pistorello, L. Artico, L. Atti-Serafini, S. Echeverrigaray, Antibacterial activity of the essential oils of *Salvia officinalis* L. and *Salvia triloba* L. cultivated in South Brazil, Food Chem., 100 (2007) 603–608.
12. G. Topçu, Bioactive Triterpenoids from *Salvia* Species, J. Nat. Prod., 69 (2006) 482–487.
13. B. Tepe, M. Sokmen, H.A. Akpulat, A. Sokmen, Screening of the antioxidant potentials of six *Salvia* species from Turkey, Food Chem., 95 (2006) 200–204.
14. C. Dincer, A. Topuz, H. Sahin-Nadeem, K.S. Ozdemir, I.B. Cam et al., A comparative study on phenolic composition, antioxidant activity and essential oil content of wild and cultivated sage (*Salvia fruticosa* Miller) as influenced by storage, Ind. Crops Prod., 39 (2012) 170–176.
15. V. Papageorgiou, C. Gardeli, A. Mallouchos, M. Papaioannou, M. Komaitis, Variation of the chemical profile and antioxidant behavior of *Rosmarinus officinalis* L. and *Salvia fruticosa* Miller grown in Greece, J. Agric. Food Chem., 56 (2008) 7254–7264.
16. M. Ijaz, M. Zafar, T. Iqbal, Green synthesis of silver nanoparticles by using various extracts: a review, Inorg. Nano-Metal Chem., 51 (2021) 744–755.
17. C.M. Nicolescu, R.L. Olteanu, M. Bumbac, Growth Dynamics Study of Silver Nanoparticles Obtained by Green Synthesis using *Salvia officinalis* Extract, Anal. Lett., 50 (2017) 2802–2821.
18. M.E. Taghavizadeh Yazdi, M. Modarres, M.S. Amiri, M. Darroudi, Phyto-synthesis of silver nanoparticles using aerial extract of *Salvia leriifolia* Benth and evaluation of their antibacterial and photo-catalytic properties, Res. Chem. Intermed., 45 (2019) 1105–1116.
19. R.R.A.L. Prabha, AgNPs Synthesis, Characterization and Antibacterial Activity from *Salvia splendens* Sellow ex Roem. & Schult. Plant Extract, Int. J. Sci. Res., 4 (2015) 1086–1090.
20. R.R.A.L. Prabha, Green Synthesis of AgNPs, Characterization and Antibacterial Activity from *Salvia Leucantha* Cav. Plant Aqueous Extract, Int. J. Sci. Res., 5 (2016) 1515–1519.
21. J.L. Lopez-Miranda, M.A. Vázquez González, F. Mares-Briones, J.A. Cervantes-Chávez, R. Esparza, G. Rosas, R. Pérez, Catalytic and antibacterial evaluation of silver nanoparticles synthesized by a green approach. Res Chem Intermed 44 (2018) 7479–7490.
22. S. Ghezi, B. Mahdavi, B. Maleki, Green Synthesis of Silver Nanoparticles Using Aqueous Extract of *Salvia Limbata*, (2016).
23. M.E. Barbinta-Patrascu, N. Badea, C. Ungureanu, D. Besliu, S. Antohe, Bioactive phyto-nanosilver particles 'green' synthesized from clary sage, burdock, southernwood and asparagus Rom. Reports Phys., 72 (2020).
24. J.H. Lee, P. Velmurugan, J.H. Park, K. Murugan, N. Lovanh et al., A novel photo-biological engineering method for *Salvia miltiorrhiza*-mediated fabrication of silver nanoparticles using LED lights sources and its effectiveness against *Aedes aegypti* mosquito larvae and microbial pathogens, Physiol. Mol. Plant Pathol., 101 (2018) 178–186.
25. W. Chartarrayawadee, P. Charoensin, J. Saenma, Rin T, Khamai P et al., "Green synthesis and stabilization of silver nanoparticles using *Lysimachia foenum-graecum* Hance extract and their antibacterial activity," Green Process. Synth., 9 (2020) 107–118.
26. V. Kumar, D.K. Singh, S. Mohan, S.H. Hasan, Photo-induced biosynthesis of silver nanoparticles using aqueous extract of *Erigeron bonariensis* and its catalytic activity against Acridine Orange, J. Photochem. Photobiol. B Biol., 155 (2016) 39–50.
27. A.K. Mittal, A. Kaler, U.C. Banerjee, Free Radical Scavenging and Antioxidant Activity of Silver Nanoparticles Synthesized from Flower Extract of *Rhododendron dauricum*," Nano Biomed. Eng., 4 (2012) 118–124.
28. I.R. Bunghez, M.E.B. Patrascu, N. Badea, S.M. Doncea, A. Popescu, R.M. Ion, Antioxidant silver nanoparticles green synthesized using ornamental plants, J. Optoelectron. Adv. Mater., 14 (2012) 1016–1022.
29. S.N. Kharat, V.D. Mendhulkar, Synthesis, characterization and studies on antioxidant activity of silver nanoparticles using *Elephantopus scaber* leaf extract, Mater. Sci. Eng. C, 62 (2016) 719–724.
30. R.S. Priya, D. Geetha, P.S. Ramesh, Antioxidant activity of chemically synthesized AgNPs and biosynthesized *Pongamia pinnata* leaf extract mediated AgNPs – A comparative study, Ecotoxicol. Environ. Saf., 134 (2016) 308–318.

31. A. Akbal, M.H. Turkdemir, A. Cicek, B. Ulug, Relation between Silver Nanoparticle Formation Rate and Antioxidant Capacity of Aqueous Plant Leaf Extracts, J. Spectrosc., 2016 (2016) 1–6.
32. P. Maisuthisakul, M. Suttajit, R. Pongsawatmanit, Assessment of phenolic content and free radical-scavenging capacity of some Thai indigenous plants, Food Chem., (2007).
33. Z.C. Arıtuluk, I.I. Tatlı Çankaya, A.M. Gençler Özkan, Antioxidant activity, total phenolic and flavonoid contents of some *Tanacetum* L. (*Asteraceae*) taxa growing in Turkey, Fabad J. Pharm. Sci., 41 (2016) 17–25.
34. S.L. Smitha, D. Philip, K.G. Gopchandran, Green synthesis of gold nanoparticles using *Cinnamomum zeylanicum* leaf broth, Spectrochim. Acta Part A Mol. Biomol. Spectrosc., 74 (2009) 735–739.
35. C.R.B. Lopes, L.C. Courrol, Green synthesis of silver nanoparticles with extract of *Mimusops coriacea* and light, J. Lumin., 199 (2018) 183–187.
36. Z. Bao, C.Q. Lan, Mechanism of light-dependent biosynthesis of silver nanoparticles mediated by cell extract of *Neochloris oleoabundans*, Colloids Surf B Biointerfaces, 170 (2018) 251–257.
37. M. Ben Farhat, A. Landoulsi, R. Chaouch-Hamada, J.A. Sotomayor, M.J. Jordán, Characterization and quantification of phenolic compounds and antioxidant properties of *Salvia* species growing in different habitats, Ind. Crops Prod., 49 (2013) 904–914.
38. M.S. Brewer, Natural Antioxidants: Sources, Compounds, Mechanisms of Action, and Potential Applications, Compr. Rev. Food Sci. Food Saf., 10 (2011) 221–247.
39. G. Agati, P. Matteini, A. Goti, M. Tattini, Chloroplast-located flavonoids can scavenge singlet oxygen, New Phytol., 174 (2007) 77–89.
40. A. Chahardoli, N. Karimi, A. Fattahi, *Nigella arvensis* leaf extract mediated green synthesis of silver nanoparticles: Their characteristic properties and biological efficacy, Adv. Powder Technol., 29 (2018) 202–210.
41. A. Chahardoli, F. Qalekhani, Y. Shokoohinia, A. Fattahi, Biological and Catalytic Activities of Green Synthesized Silver Nanoparticles from the Leaf Infusion of *Dracocephalum kotschyi* Boiss, Glob. Challenges, 5 (2021) 2000018.
42. B.A. Chopade, R. Singh, P. Wagh, S. Gaidhani, A. Kumbhar et al., Synthesis, optimization, and characterization of silver nanoparticles from *Acinetobacter calcoaceticus* and their enhanced antibacterial activity when combined with antibiotics, Int. J. Nanomedicine, 8 (2013) 4277.
43. J.L. López-Miranda, J.A. Cervantes-Chávez, A.R. Hernández-Martínez, R. Pérez, R. Esparza, M. Estévez-González, Study on the photocatalytic and antibacterial properties of silver nanoparticles synthesized by a green approach, Mater. Res. Express, 6 (2019) 065066.
44. S.A. Cherrak, N. Mokhtari-Soulimane, F. Berroukeche, B. Bensenane, A. Cherbonnel et al., In Vitro Antioxidant versus Metal Ion Chelating Properties of Flavonoids: A Structure-Activity Investigation, PLoS One, 11 (2016) e0165575.
45. M. Muti, A. Erdem, A. Caliskan, A. Sınag, T. Yumak, Electrochemical behaviour of carbon paste electrodes enriched with tin oxide nanoparticles using voltammetry and electrochemical impedance spectroscopy, Colloids Surfaces B Biointerfaces, 86 (2011) 154–157.
46. S. Ortaboy, Electrochemistry and sensitive determination of a metal complex azo dye using graphite paste electrode modified with Na-bentonite, J. Turkish Chem. Soc. Sect. A Chem., 4 (2017) 931–952.